ELSEVIER

Journal of Nuclear Materials 313–316 (2003) 1167–1172

journal of nuclear materials

www.elsevier.com/locate/jnucmat

Flow measurements in the scrape-off layer of Alcator C-Mod using impurity plumes

S. Gangadhara *, B. LaBombard

M.I.T. Plasma Science and Fusion Center, 175 Albany St., NW 17-125, Cambridge, MA 02139, USA

Abstract

Accurate measurements of plasma flows in the scrape-off layer (SOL) are a necessary requirement for understanding the physics of tokamak edge plasmas. A system is being developed on Alcator C-Mod for inferring flows parallel ($v_{\|}$) and perpendicular ($v_{\mathbf{E}\times\mathbf{B}}$) to local magnetic field lines from impurity emission patterns ('plumes') generated by local gas injection. Carbon plumes are generated at variable location in the SOL by puffing deuterated ethylene gas (C_2D_4) through the end of a reciprocating fast-scanning probe. Two intensified CCD cameras are used to record C^{+1} and C^{+2} emission patterns simultaneously from near-perpendicular views. Plumes are modeled using a Monte Carlo impurity transport code, from which values for the background flows may be extracted. The sensitivity of the plume structure is investigated for a number of code inputs, including radial electric field ($\mathbf{E}_r$) and the neutral launch dynamics. Initial modeling results indicate discrepancies between values of $v_{\|}$ and $\mathbf{E}_r$ extracted from the plumes and measurements obtained from probe data.

PACS: 52.70.K; 52.25.V; 52.65.P; 52.55.F
Keywords: Scrape-off layer flows; Visible imaging; Impurity plumes; Monte Carlo methods; Alcator C-Mod

1. Introduction

Flows parallel and perpendicular to local magnetic field lines play an important role in tokamak edge plasmas. Accurate measurements of flows in the scrape-off layer (SOL) are therefore desired. On Alcator C-Mod, reciprocating fast-scanning probes are typically used to make measurements of parallel flows ($v_{\|}$) and radial electric fields ($\mathbf{E}_r$) in the SOL. Interesting conclusions about edge plasma physics result from the interpretation of these measurements. For example, recent results [1] indicate that over much of the SOL cross-field transport to the main-chamber walls dominates over parallel transport to the divertor, a result based in part on the measurement of low parallel flow velocities in the SOL. Reversed flows, or flows away from the divertor, are also measured near the separatrix of most C-Mod discharges [2]. Depending on the magnitudes of $v_{\|}$ and $\mathbf{E}_r$, impurities generated near divertor surfaces may be transported into the main-chamber SOL, providing a mechanism of enhancing impurity concentrations in the core plasma.

An independent measurement of SOL flows is available by viewing impurity emission patterns ('plumes') generated by localized injection of gas into the edge plasma. A system has been developed on Alcator C-Mod to inject impurity gas at variable distance from the separatrix, up to the last-closed flux surface (LCFS), via the reciprocating F-port scanning probe (FSP) [3]. Plasma flows are inferred from modeling the resulting impurity emission plumes, imaged from two near-perpendicular views. Measurements of the local electron density and temperature are also provided by the probe, and are used in plume modeling.

Experiments employing impurity gas injection through the FSP have previously been conducted on Alcator C-Mod [4]. Recent modifications to this

* Corresponding author. Tel.: +1-617 253 5401; fax: +1-617 253 0627.
E-mail address: sanjayg@psfc.mit.edu (S. Gangadhara).

0022-3115/03/$ - see front matter
PII: S0022-3115(02)01515-5

experimental technique include the use of beam-splitter optics for the simultaneous acquisition of C^{+1} and C^{+2} emission and simulation of plume emission using a 3-D Monte Carlo transport code [5]. In this paper, we report on initial results from this upgraded system and progress towards its development for inferring SOL flows from the dispersal of C^{+1} and C^{+2} plumes.

2. Experimental arrangement

A cross-section of the Alcator C-Mod vacuum chamber with a layout of the main diagnostics for the gas-injection system is shown in Fig. 1. This system consists of two near-perpendicular views of a reciprocating fast-scanning probe designed to inject gas locally into the SOL at the probe's end-of-stroke. For these experiments deuterated ethylene (C_2D_4) was used as the working gas, with $\sim 5 \times 10^{16}$ molecules of gas typically injected per probe scan. The probe head is machined from a molybdenum cylinder and has four tungsten electrodes. Views are obtained using fiber optic bundles coupled to gated, intensified CCD cameras through beam-splitter optics. The majority of this system is described in detail in [4] – the new features are the beam-splitters, composed of mirrors, lenses, and bandpass interference filters, which allow for the simultaneous acquisition of C^{+1} (CII) and C^{+2} (CIII) emission at each view location.

3. Initial results

3.1. Plume emission patterns in the near and far SOL

False color images of CII (514.1 nm) and CIII (465.0 nm) emission recorded by the CCD cameras are shown in Fig. 2 for a pair of ohmic L-mode discharges taken at different depths in the SOL. In the side view (SVC), emission is partly obscured by the probe head, while in the top view (TVC) the probe head contributes some reflected light. A schematic of the probe head is shown in each SVC figure, and the FSP nozzle location is indicated in each TVC figure.

Asymmetries exist in both the parallel and cross-field structure of plume emission. Parallel asymmetries are related to background parallel flows, and the nature of these asymmetries is seen to vary with distance in the SOL (far SOL – strong asymmetry indicating flow towards the divertor; near SOL – asymmetry indicating reversed flow). In the cross-field direction, it is observed that the tails of the emission are bent further off of the

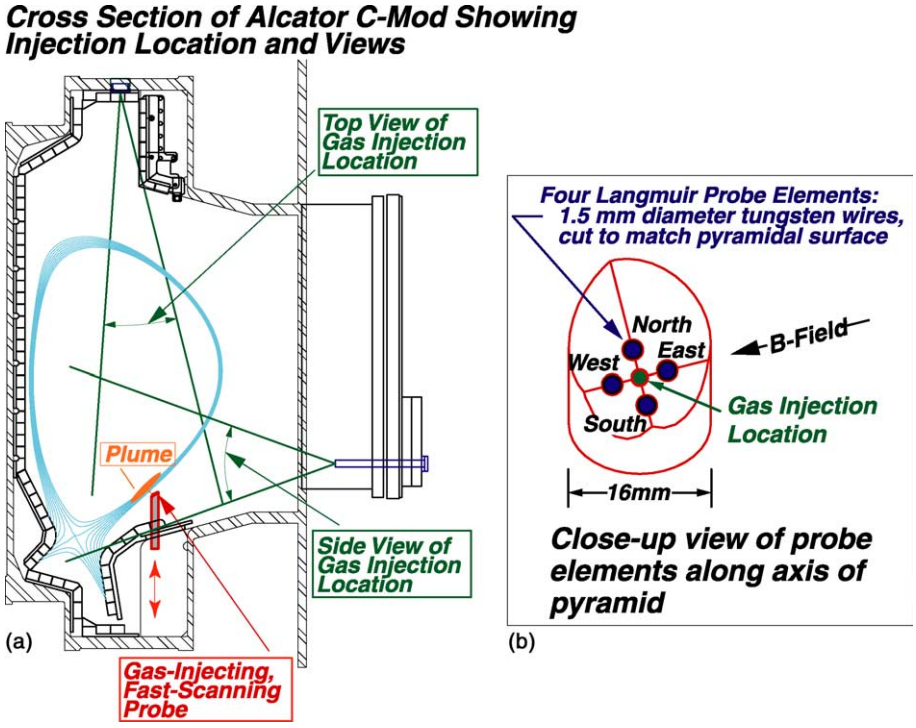

Fig. 1. (a) Cross-section of the Alcator C-Mod vacuum chamber with a typical diverted equilibrium. Gas is injected locally into the SOL at the end of stroke of a vertically-scanning probe. Impurity emission plumes are viewed from two near-perpendicular locations. (b) Close-up view of molybdenum probe head, indicating the location of the gas-injection capillary and the Langmuir probe elements used for density and temperature measurements and for providing estimates of the background flow.

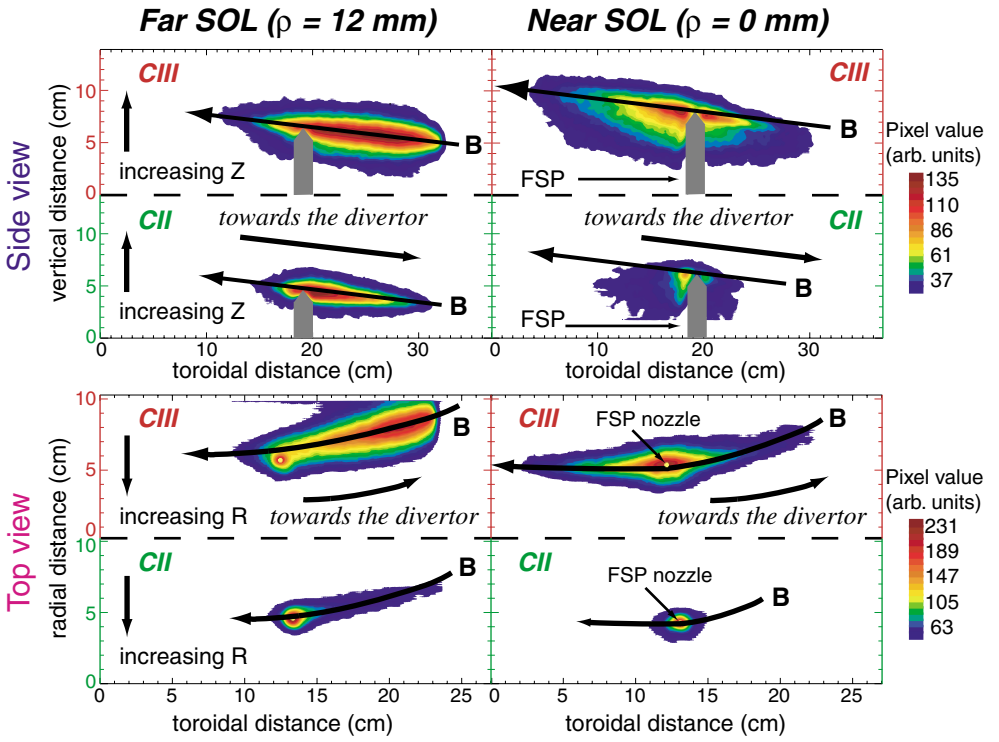

Fig. 2. Smoothed CII (514.1 nm) and CIII (465.0 nm) emission data from the SVC and TVC. Both data were taken during ohmic L-mode discharges. Data on the left were taken at a position in the far SOL, whereas data on the right were taken at the separatrix (indicated by ρ, which represents distance across flux surfaces mapped to the midplane). A schematic of the probe head is drawn in each SVC figure to indicate its perturbance, as well as to show the gas injection location (probe tip). In each TVC figure the gas injection location is given by the FSP nozzle position. An approximate local magnetic field direction is indicated to orient the emission. Note that emission (characterized by pixel value) for the TVC is larger than for the SVC, due to the contribution of reflected light from the probe head.

axis of emission as distance is increased from the injection location. This 'boomerang' effect is thought to be due to the $\mathbf{E} \times \mathbf{B}$ drift of impurity ions resulting from the presence of a radial electric field in the SOL. This effect is rather weak for plumes in the far SOL, but can be much stronger for plumes near the separatrix. In both cases the direction of the boomerang implies that $\mathbf{E}_r$ is directed radially outward, i.e. $\mathbf{E}_r > 0$. This is true for the majority of plumes studied.

3.2. Carbon source distribution

Experimental results suggest that two sources of carbon contribute to plume formation – carbon ions formed from prompt breakup of C_2D_4 gas and carbon sputtered from a deposited layer on the probe head. A close-up view of an experimental CIII TVC plume (mapped to field-aligned coordinates using the EFIT magnetic reconstruction code [6]) is shown in Fig. 3 (top panel). A simulated plume (to be discussed in Section 4.3) is shown in the bottom panel.

The experimental emission pattern is characterized by large cross-field width and 'jet'-like behavior. Based on the injection capillary diameter (1 mm), and typical diffusivities ($D_\perp \sim 0.1$–1 m^2/s) and ionization times ($\tau_{ion} \sim 1$–10 μs) for C^{+2} ions in the SOL, the cross-field width of CIII plumes is expected to be ~1–3 mm. However, the cross-field dimension of the experimental emission is typically larger than this (Fig. 3, top panel). Effective cross-field widths are determined from a moment analysis of the emission (with data corrupted by the prescence of the probe ignored), and are typically ~7–10 mm. These values would be consistent with plume emission generated from sputtering of re-deposited carbon on the molybdenum probe head. Experimental evidence for this exists in the form of plumes generated in a discharge *without* gas injection following a discharge with gas injection. Near the gas injection location (along **B**), plumes exhibit a jet-like structure, as particles in the shadow of the probe seem to flow more strongly away from the probe than particles outside the probe shadow. This behavior is related to the injection

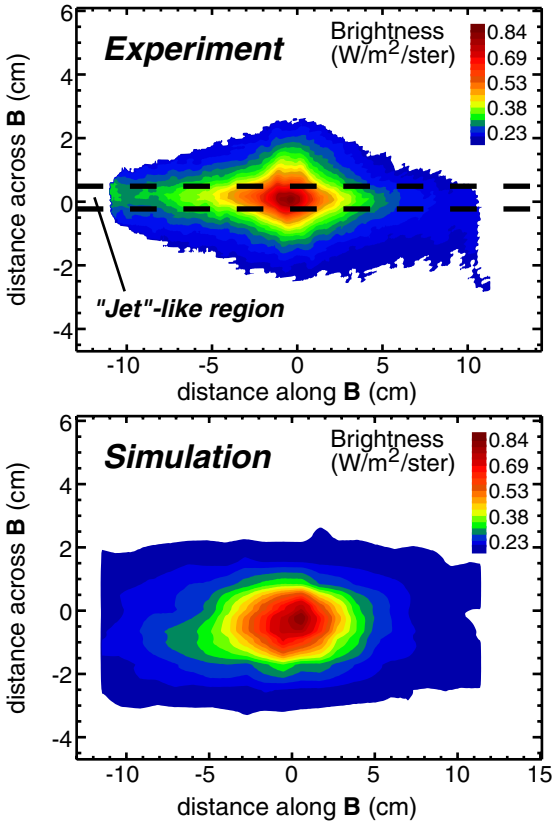

Fig. 3. Comparison between experimental and simulated CIII TVC plumes. Top panel: CIII TVC plume generated at the separatrix during discharge 1001012006, 950 ms ($n_e = 1.14 \times 10^{20}$ m^{-3}, $T_e = 60$ eV). Emission has been absolutely calibrated and mapped to field-aligned coordinates using the EFIT reconstruction code. Bottom panel: Simulated CIII TVC plume. Density and temperature profiles measured by the scanning probe for discharge 1001012006, 950 ms are used in the simulation. Code inputs are: $M_\parallel = -0.46$ (constant over source region); $v_\perp = 2.2$ km/s (towards the divertor) at the injection location, corresponding to $\mathbf{E}_r = 11$ kV/m for this discharge; λ (=source e-folding length) = 1.2 cm; U_0 (=surface binding energy) = 20 eV; $D_\perp = 1$ m^2/s.

source, as it is not seen in plumes generated without gas injection. In this paper, we focus on the development of a sputter source model of the plume emission to simulate the overall extent of the carbon dispersal (the issue of the jet is revisited later).

4. Plume modeling

4.1. Impurity transport model

Extraction of plasma flows from emission data requires modeling of the plume structure. This is done using LIM [5], a 3-D Monte Carlo code describing the transport of impurities generated from a limiter surface. Inputs to the code include background transport parameters ($v_\parallel, v_\perp \propto \mathbf{E}_r, D_\perp$), as well as background density and temperature profiles, in this case obtained from probe measurements. The primary outputs of the code are 3-D density distributions for each impurity charge state. Numerical simulations of the camera views are used to image the simulated emission, producing 2-D brightness data which can be directly compared with experimental results. Transport parameters are then varied to obtain a match between simulation and experiment.

Plumes are simulated using a sputter source model – neutral carbon atoms are launched from the probe surface with a Thompson velocity distribution relative to the local surface normal [7]. The surface binding energy, U_0, is specified as a code input. The source strength is assumed to vary exponentially with distance from the injection location along the probe axis – the e-folding length, λ, is also a code input.

4.2. Sensitivity study

Sensitivity studies have been conducted to investigate the affect various code parameters have on the overall plume shape. An example of the affect of finite poloidal flow (due to $\mathbf{E} \times \mathbf{B}$ drifts) on simulated CIII TVC plumes is shown in Fig. 4. Typical density and temperature profiles near the separatrix for a medium density ohmic L-mode discharge are assumed. In the top panel, no poloidal flow is given in the simulation. Nonetheless, the emission exhibits a boomerang shape consistent with $\mathbf{E}_r < 0$. This boomerang arises because of the radial variation of the ionization rate, which causes a radial skewness in the impurity density. This skewness is towards regions of low n_e and T_e, i.e. outward in major radius as seen from the top view and vertically downwards as seen from the side (not shown). In the bottom panel a poloidal flow profile has been inputted, with flow directed towards the divertor, ($\mathbf{E}_r > 0$; $v_{\mathbf{E}\times\mathbf{B}}$ at the injection location = 2250 m/s), causing the plume boomerang to change direction. For $\mathbf{E}_r > 0$, the boomerang resulting from the poloidal skewness in the plumes is radially inwards when seen from the top view and vertically downwards when seen from the side. Thus, when $\mathbf{E}_r$ is positive, the effect of ionization rate variation is to increase the plume boomerang in the side view and to decrease the boomerang (or change its direction if $\mathbf{E} \times \mathbf{B}$ drifts are small) in the top view.

Other effects found to have a significant influence on the plume shape include the presence of flows and electric fields in the presheath and the neutral source e-folding length. Presheath fields tend to reduce the effective parallel velocity of impurities away from the probe, causing the parallel emission profile to be more peaked and the plume boomerang to increase. As the

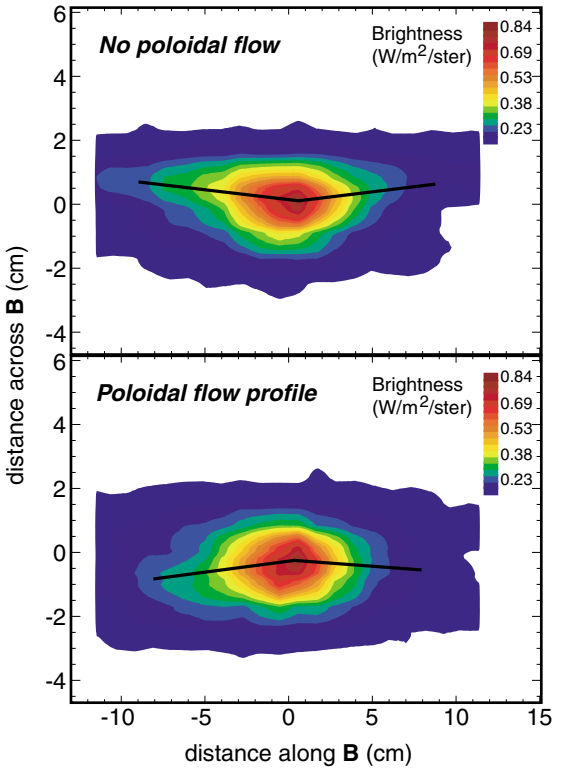

Fig. 4. Simulated CIII top view plumes for cases with and without poloidal flows. Density and temperature profiles near the separatrix for a typical medium density, ohmic L-mode discharge are used. Top panel: No poloidal flow. The boomerang is due to the radial skewness in the impurity density resulting from the radial variation of the ionization rate. Bottom panel: Poloidal flow profile, with flows directed towards the divertor ($\mathbf{E}_r > 0$) and a value of 2250 m/s at the injection location. Both poloidal flow (due to $\mathbf{E} \times \mathbf{B}$ drifts) and radial ionization rate variation contribute to the overall boomerang in the plume.

neutral source e-folding length, λ, is increased, the cross-field width and parallel asymmetry in the plume emission are also seen to increase. This results from the pyramidal probe shape yielding a larger source size with increased λ, and a larger fraction of neutrals consequently being launched in regions of colder and less dense plasma, where ionization rates are decreased and coulomb momentum transfer cross-sections are increased. These particles have a longer effective lifetime and are more strongly coupled to the background plasma, allowing them more opportunity to cross-field diffuse and to acquire the background flow velocity.

4.3. Simulation of experimental data

LIM has been used to simulate an experimental CIII TVC plume generated at the separatrix during an ohmic L-mode discharge ($n_e = 1.14 \times 10^{20}$ m^{-3}, $T_e = 60$ eV). False color images of the experimental and simulation results are shown in Fig. 3. Input parameters for this case are: $M_\parallel = -0.46$ (constant over the source region); $v_\perp = 2.2$ km/s (towards the divertor) at the injection location, corresponding to $\mathbf{E}_r = 11$ kV/m for this discharge; $\lambda = 1.2$ cm; $U_0 = 20$ eV; $D_\perp = 1.0$ m^2/s.

Based on these results, a net poloidal flow can be calculated, by summing together the poloidal projection of the parallel flow ($v_\parallel B_\theta / B$) with the $\mathbf{E} \times \mathbf{B}$ flow. For this case the result is $v_{\theta,net} = -2$ km/s, implying a net poloidal flow *away* from the divertor. However, other measurements on Alcator C-Mod suggest that near the separatrix the net poloidal flow velocity is small, i.e. that to a large degree the poloidal projection of the parallel flow cancels the $\mathbf{E} \times \mathbf{B}$ flow [2]. In addition, the values for $M_\parallel$ and $\mathbf{E}_r$ disagree with those measured by the scanning probe: $M_{\parallel,\mathrm{probe}} = -0.2$, $\mathbf{E}_{r,\mathrm{probe}} = -20$ kV/m. What are the causes for these discrepancies?

One problem is the inability of the simulated plumes to re-create the jet-like behavior seen in the experiment. As mentioned previously, this phenomenon is related to the direct injection source, which is not presently being modeled in LIM. This jet results in broad parallel profiles in the emission – to simulate the overall extent of the plume without a jet, an artificially high value of U_0 (surface binding energy) is required, which results in the average speed of particles away from the injection location also being large. To match the parallel asymmetry in the experimental emission, a large background flow is then necessary. Incorrect modeling of the source profile may also affect what cross-field flows are required to match the plume boomerang, leading to errors in $\mathbf{E}_r$.

In addition, the plumes exist over a finite volume, and values for $v_\parallel$ and $\mathbf{E}_r$ inferred from the emission structure are averages weighted by the impurity distribution. Difficulties may arise in comparing these values with localized measurements from the scanning probe.

The probe measures $\mathbf{E}_r < 0$ for this case, whereas plume modeling implies $\mathbf{E}_r > 0$. Regardless of whether the magnitude of $\mathbf{E}_r$ is correctly assessed by the modeling, the direction of the experimental boomerang implies that $\mathbf{E}_r$ must be positive. This result suggests the probe measurement is incorrect. Probe measurements of $\mathbf{E}_r$ involve taking the derivative of the local plasma potential, which itself involves summing the sheath potential (inferred by multiplying the electron temperature by a scale factor) with the floating potential. Near the separatrix these are large offsetting quantities, so that their sum may be subject to large errors. Recently, a comparison of $\mathbf{E}_r$ inferred from fluctuation propagation velocities with that inferred from probe-sheath potential drop has been performed [2] – results suggest that the latter technique may be unreliable. Thus, near the separatrix the plumes may provide a more reliable measurement of $\mathbf{E}_r$.

5. Summary

A novel system has been developed for determining flows in the SOL of Alcator C-Mod. A reciprocating FSP has been designed to inject gas locally in the SOL, while two near-perpendicular views of the probe provide images of the resulting impurity dispersal plumes. Parallel and cross-field flows are inferred from modeling the dimension and structure of the plumes. Experimental results suggest that both the direct injection source and sputtering of re-deposited carbon on probe head contribute to the plume emission. Modeling thus far has focused on development and implementation of a sputter source.

A Monte Carlo impurity transport code is used to model the plume emission, and to investigate which parameters affect plume structure. Plume shape is found to be sensitive to radial variations in the impurity ionization rate. These variations result in a boomerang in the emission, which adds to or subtracts from the boomerang due to $\mathbf{E} \times \mathbf{B}$ flows, depending on the sign of $\mathbf{E}_r$ and the geometry of the view. Plume structure has also been found to depend on presheath physics and neutral launch dynamics.

Simulation of an experimental plume has been performed, allowing $v_\parallel$ and $\mathbf{E}_r$ to be extracted from the emission data. These results do not compare well with those obtained from probe measurements. This may be due to jet-like behavior observed in the experimental plume emission which is not presently modeled. Averaging resulting from the finite emission volume may also lead to discrepancies between plume results and probe measurements. Finally, there is evidence that the probe measurement of $\mathbf{E}_r$ is incorrect. From the direction of the plume boomerang, the sign of $\mathbf{E}_r$ can be directly inferred – for the case studied, this value is positive, which is inconsistent with the probe estimate of $\mathbf{E}_r$. In this regard, the plumes may ultimately provide a more robust measurement of this quantity near the separatrix region.

Acknowledgements

The authors would like to thank David Elder and Steve Lisgo at the University of Toronto for their assistance with LIM modeling. This work is supported by US Department of Energy Contract no. DE-AC02-78-ET-51013.

References

[1] B. LaBombard, M.V. Umansky, et al., Nucl. Fusion 40 (2000) 2041.
[2] B. LaBombard et al., these Proceedings. PII: S0022-3115(02)01435-6.
[3] B. LaBombard, S. Gangadhara, et al., J. Nucl. Mater. 266–269 (1999) 571.
[4] S. Gangadhara, B. LaBombard, et al., J. Nucl. Mater. 290–293 (2001) 598.
[5] P.C. Stangeby et al., Nucl. Fusion 28 (1988) 1945.
[6] L.L. Lao et al., Nucl. Fusion 25 (1985) 1611.
[7] R.A. Langley et al., in: Data Compendium for Plasma–Surface Interactions, Nucl. Fusion Special Issue, IAEA, Vienna, 1984, p. 61.